Research note

Comparison of the Performance of Different Thermodynamic Models for Liquid Phase in Predicting the Phase Behavior of Hydrogen Hydrates with THF

M. Ghorbanzadeh, C. Ghotbi[*], V. Taghikhani
Department of Chemical and Petroleum Engineering, Sharif University of Technology, Tehran, Iran

Abstract
In this work, five different thermodynamic models for correlating the fugacity of water and Tetrahydrofuran (THF) in liquid phase in equilibrium with hydrogen hydrate phase, based on the van der Waals–Platteeuw (vdW-P) statistical thermodynamic model are used and the equilibrium pressures of hydrogen hydrate at different temperatures are calculated. The dissociation pressure of binary hydrogen hydrates is determined by using the Zele–Lee–Holder cavity distortion model. The studied models in liquid phase are NRTL excess Gibbs energy, Peng-Robinson (PR) equation of state (PR EOS), Peng-Robinson-Steryjek-Vera EOS with the Wong-Sandler mixing rule (PRSV-WS), Dashtizadeh EOS (DPTG), and Ghotbi-Vera Simple SAFT (GV-SSAFT) EOS. The results show that the GV-SSAFT model correlates more accurately the experimental dissociation pressure of binary hydrogen hydrate. Additionally, hydrogen storage capacity of binary hydrogen hydrates is calculated.

Keywords: *Hydrogen Hydrate, GV-SSAFT EOS, Water-THF Solution, Lattice Distortion Model*

1. Introduction

Hydrogen has great potential as an energy source for a number of reasons; the energy produced by oxidation per unit of mass of hydrogen (142 MJ/kg) is at least three times larger than that of other chemical fuels. Its oxidation product is water and, in addition, hydrogen can be generated from renewable sources in a closed system. For this reason, technologies for using hydrogen as an alternative fuel in automotive applications are under continuous development. One of the main technological challenges in the implementation of these technologies is the development of a safe and efficient way of storing hydrogen [1]. The aim of hydrogen storage technologies is to reduce the volume that hydrogen naturally occupies in its thermodynamically stable state under ambient conditions, i.e., as a gas. Hydrogen gas shows a very low density (0.089 kg/m^3), which means that only a little mass is

---

∗ Corresponding author: ghotbi@sharif.edu

contained within a large volume of gas. However, hydrogen shows a very high energy content by weight, and thus, an interesting fuel or energy carrier. Therefore, it is necessary to transform hydrogen into an easily handled form, e.g., by compression or liquefaction, or by trapping through interaction with other compounds by means of strong or weak interactions such as covalent bonds or van der Waals interactions [2]. For example, in conventional high-pressure tanks (usually filled up to 200 bar), the volume required to store hydrogen is as high as 56 L/kg. This volume can be reduced if hydrogen is stored as a liquid, but in this case, cryogenic temperatures are required (-253°C at 1 bar). Moreover, the energy cost of compressing and cooling down the gas is very high, and thus, this option becomes very expensive, and it is not practical for everyday use. Other possibilities include adsorption of gaseous hydrogen on solid surfaces of carbon and the use of metal hydrides, with conflicting results about the reversibility of the process, that is, the possibility of releasing all of the hydrogen that was stored in the carbon or in the hydride, and the energy storage density [1].

One of the paths currently being investigated by researchers for hydrogen storage is the use of clathrate hydrates. Clathrates (gas) hydrates are crystalline solids composed of water and gas. The gas molecules (guests) are trapped in water cavities (host) that are composed of hydrogen-bonded water molecules [3]. Depending on the size and shape of the guest's molecules, water molecules form different cages that combine to form the hydrates of the three different crystallographic structures, I, II, and H [4].

Small molecules such as argon form sII hydrates $[8(5^{12}6^4)\cdot16(5^{12})\cdot136H_2O]$, whereas larger molecules like methane form sI $[6(5^{12}6^2)\cdot2(5^{12})\cdot46H_2O]$. Even larger molecules like tetrahydrofuran (THF) form sII. The largest hydrate guests (~7–9 Å) form sH hydrate $[1(5^{12}6^8)\cdot2(4^35^66^3)\cdot3(5^{12})\cdot34H_2O]$ with the help of another smaller molecule like methane [5].

Historically the hydrogen molecule was considered to be too small to contribute to the stability of clathrate hydrates. That is, in gas mixtures containing hydrogen, hydrogen was thought to be a diluent for other natural gas components rather than a hydrate forming molecule [5]. However, in 1999, Dyadin *et al.* discovered for the first time that hydrogen can form clathrate hydrates at high pressures (up to 1.5GPa) [6].

In 2002, Mao *et al.* performed the first detailed molecular study on the $H_2 + H_2O$ system under pressure (300MPa at 350 K). They confirmed pure H_2 clathrate hydrate formed sII with a lattice parameter of 17.047 Å [7]. Mao *et al.* synthesized a hydrogen clathrate hydrate, $H_2 (H_2O)_2$, that holds 50 g/lit hydrogen by volume or 5.3 wt %. They suggested that pure hydrogen hydrate is stabilized with double and quadruple occupancy of hydrogen molecules in the small and large cages of sII hydrate, respectively [8]. The clear disadvantage to using hydrogen hydrate as a storage material is the high pressure required for formation (200MPa at 273K) [5]. In an attempt to lower the pressures necessary for hydrogen hydrate formation, Florusse *et al.* showed that hydrogen clusters can be stabilized and stored at low pressures (5MPa at 280K) by stabilizing the large water cages with a

second guest component (promoter), tetrahydrofuran [9]. Florusse *et al*. predicted that in the case of sII binary hydrogen hydrate, with double occupancy of the small cavities by H_2 and the large cavities partially occupied by THF, the mass of hydrogen could be up to 4wt% [9]. One disadvantage of promoter is that it occupies large cavities that result in decreasing hydrogen storage capacity. In 2005 Lee *et al*. [10] showed that stoichiometric THF/H_2 contains two hydrogen molecules per small cavity. They suggested by decreasing the concentration of THF a hydrate could be formed in which large cavities were only partially occupied by THF and clusters of four hydrogen molecules could be stored in vacant large cavities. Using this approach, Lee *et al*. presented evidence for a nonstoichiometric THF + H_2 hydrate that contained about 4 wt. % H_2 at conditions of 12MPa and 270K. In contrast to the double occupancy suggestion by Lee *et al*., several studies have suggested that hydrogen storage is independent of THF composition and maximum amount of H_2 in THF+H_2 is 1wt% ([11] [12] [13]).

Theoretical analyses of the formation conditions and properties of hydrogen hydrates are useful tools that can complement experimental data and help to answer questions. After determination of the hydrate crystal structures in the early 1950s, it was possible to generate theories for equilibria of macroscopic properties based upon microscopic properties. The initial statistical thermodynamic model was generated by Barrer and Stuart (1957), with a more accurate method by van der Waals and Platteeuw (1959), who are considered the founders of the method [3]. This model is

based on the following assumptions:

1. Each cavity can only contain one guest molecule.
2. There are no interactions of the guest molecules.
3. Encaged molecules do not distort the cavity.
4. Classical statistics are valid.

Several studies modified the assumptions of van der Waals–Platteeuw model.

In the present study, equilibrium conditions of binary hydrogen hydrates with THF as a promoter at different temperatures and pressures are calculated with Zele–Lee–Holder cavity distortion model. Five different thermodynamic models for correlating the fugacity of water and Tetrahydrofuran (THF) in liquid phase in equilibrium with hydrogen hydrate phase are employed and then performances are compared. The studied models are selected from different and well known groups of equations.

2. Theory

Lattice distortion model modified some assumptions of vdW-P model as follows [14].

1. The cavity is not rigid and can be distorted due to the size of the host molecule
2. There is nonlinear composition based distortion in hydrates formed from mixtures.

When the hydrate phase is in equilibrium with the water phase, the chemical potential for both phases is the same.

$$\mu_W^H = \mu_W^L \Leftrightarrow \Delta\mu_W^{\beta-H} = \mu_W^\beta - \mu_W^H = \mu_W^\beta - \mu_W^L = \Delta\mu_W^{\beta-L}$$

(1)

where μ_W^{β} is the chemical potential of the water in the empty hydrate at 0°C, zero pressure, μ_W^{H} is the chemical potential of hydrate, and μ_W^{L} is the chemical potential of water. The chemical potential difference for hydrate can be expressed by van der Waals [14]:

$$\Delta\mu_W^{\beta-H} = -RT \sum_i v_i \, ln(1-\sum_j \theta_{ji}) \qquad (2)$$

In this equation v_i is the ratio of i type cavities to the number of water molecules in hydrate phase and θ_{ji} is the fraction of the type i cavity occupied by the guest molecule j. This fractional occupancy of the cavity is expressed as:

$$\theta_{ji} = \frac{C_{ji} f_j}{1+\sum_j C_{ji} f_j} \qquad (3)$$

where C_{ji} is the Langmuir constant. Langmuir constant is solved numerically using smooth-cell potentials:

$$C_{ji} = \frac{4\pi}{kT} \int_0^{R-a} exp(-\frac{W_1(r)+W_2(r)+W_3(r)}{kT}) r^2 dr \qquad (4)$$

In equation (4) W_1, W_2 and W_3 are the smoothed-cell potential contributions of the first, second, and third shells of water [14]. Three shell radii of small and large cavity of structure II hydrates are calculated by the following equation:

$$R = a + \beta\Delta\mu_{mix}^o \qquad (5)$$

where R is a cavity radius and α and β are

shell radii parameters that were reported by Zele [15].

The three shell cavity radii are used for determining Langmuir constant according to equation (4). Promoter enters in the large cavities SII and hydrogen molecule can enter in small and large cavities ([7], [9], [10]). Exp-6 potential model is used for calculating Langmuir constant of hydrogen. Smooth cell potential form of this model is expressed by [16]:

$$W(r) = \frac{z\,\varepsilon}{2(\alpha-6)} \left[\frac{6\alpha^2}{Rr} \left[\frac{r_m}{\alpha}((R-r)e^{-\alpha(R-r)/r_m}) \right. \right.$$
$$+ \frac{r_m^2}{\alpha^2}[e^{-\alpha(R-r)/r_m}e^{-\alpha(R-r)/r_m}] \left. \right]$$
$$\left. + \frac{r_m^6}{4Rr}(\frac{1}{(R-r)^4} - \frac{1}{(R+r)^4}) \right] \qquad (6)$$

where z is coordination number, R is the cavity radius and r is the distance between a hydrogen cluster and the center of the cavity. The negative value of ε represents the minimum potential energy at a separation distance of r_m. α describes the steepness of the repulsive part. Interaction parameter ε, α and r_m were reported in the literature [16] by ab initio calculation.

Kihara potential is used for calculating Langmuir constant of THF. Smooth cell potential of this model is expressed by [17]:

$$W(r) = 2z_i\varepsilon \left[\frac{\sigma^{12}}{R_i^{11}r} \left(\delta^{10} + \frac{\alpha}{R_i}\delta^{11} \right) - \frac{\sigma^6}{R_i^5 r} \left(\delta^4 + \frac{\alpha}{R_i}\delta^5 \right) \right] \qquad (7)$$

$$\delta^N = \frac{1}{N} \left[\left(1 - \frac{r}{R_i} - \frac{\alpha}{R_i} \right)^{-N} - \left(1 - \frac{r}{R_i} - \frac{\alpha}{R_i} \right)^{-N} \right] \qquad (8)$$

The parameters needed for application of Kihara are the core radius at zero potential σ, the characteristic energy ε and the core radius α that are reported in the literature [17].

The chemical potential difference for water phase is calculated from the equation developed by Holder *et al.* [18]:

$$\frac{\Delta\mu_w}{RT} = \frac{\Delta\mu_w^o}{RT_o} - \int_{T_o}^{T} \frac{\Delta h_w}{RT^2} dT + \int_{T_o}^{P} \frac{\Delta V_w}{RT} dT - \ln\gamma_w x_w$$

(9)

$\Delta\mu_w^o$ is the difference in the chemical potential of water between the empty hydrate lattice and ice at T0 (273.15 K), Δh_w and ΔV_w are the differences in the enthalpy and the volume between the empty hydrate and pure liquid water phases, respectively, γ_w is the activity coefficient, and x_w is the mole fraction of water in the liquid water phase. These parameters were reported by Sloan [19].

The nonlinear composition assumption of lattice distortion theory is used for the calculation of the dissociation pressure of binary mixtures. Distortion for mixture gas hydrates (multi-gas component + water) is based upon a nonlinear combination of the Δh_w^o and $\Delta\mu_w^o$ for all species present. Lee – Holder [14] defined an ideal mixture with this reference chemical potential difference (RCPD):

$$\Delta\mu_{mix}^{o,ideal} = \sum_i \Delta\mu_i^o Z_i$$

(10)

where $\Delta\mu_{mix}^{o,ideal}$ is ideal reference chemical

potential difference (ideal RCPD), Zi is the water-free mole fraction of gas in hydrate phase and reference properties $(\Delta\mu_i^o)$ of THF and H2 for calculating ideal RCPD were reported by Lee *et al.* [20].

For mixture hydrates, RCPD is expressed by [14]:

$$\Delta\mu_{mix}^o = \Delta\mu_{mix}^{o,ideal} + \Delta\mu_{mix}^{o,excess}$$

(11)

With

$$\Delta\mu_{mix}^{o,excess} = Z_1 Z_2 [A + B(Z_1 - Z_2)]$$

(12)

where constant *A* and *B* are obtained from the experimental data. The water-free mole fraction of gas in hydrate phase (Z_1, Z_2) is given by:

$$Z_j = \frac{\sum_i u_i \theta_{ij}}{\sum_j \sum_i u_i \theta_{ij}}$$

(13)

An initial guess of $\Delta\mu_w^o$ is used for calculation of the three-shell radii of small and large cavities of Structure I and II hydrates by equation (5) and then Langmuir constant by equation (3). Experimental data of temperature, pressure and compositions of THF in liquid phase in equilibria with hydrate phase are used to determine the fugacity of individual components in vapor and liquid phases. Using the Langmuir constants and the fugacity of all of the components in liquid and vapor phases, the chemical potential difference of water in the hydrate phase can be calculated as given by equation (2). At equilibrium $\Delta\mu_w$ is equal to $\Delta\mu_w^H$ and all the other terms in equation (5)

are calculated except $\Delta\mu^o$. Therefore, $\Delta\mu^o_{mix}$ is calculated by an iterative procedure. A and B coefficients are determined with several values of $\Delta\mu^o_{mix}$.

2-1. Equation of state

In order to calculate fractional occupancy of the cavities, the fugacity of components in phases in equilibrium with the hydrate phase should be determined. The Peng–Robinson EOS can be used for calculating the fugacity of each component in gas phase [21].

By ignoring the solubility of H_2 in aqueous phase, the fugacity of other component in liquid phase can be calculated using different based EOS or based on excess Gibbs free energy (g^E) model.

In this work NRTL activity coefficient model [22], Peng–Robinson EOS[21], Stryjek–Vera modification of Peng–Robinson EOS with the Wong–Sandler mixing rules (PRSV-WS) [23, 24], Dashtizadeh EOS (DPTG) [25], and Ghotbi–Vera SSAFT EOS [26] are used to calculate the fugacity of each component in liquid phase. PR EOS and PRSV EOS are expressed by:

$$P = \frac{RT}{(v-b)} - \frac{\alpha_c \alpha}{[v(v-b)+b(v-b)]} \quad (14)$$

Stryjek and Vera modified α parameter in PR EOS. In Peng-Robinson EOS, Wong–Sandler mixing rules [24] are also used from the NRTL g^E model at infinite pressure. The PRSV-WS model has four empirical parameters for each binary in the mixture. Therefore, for a binary mixture the Wong–Sandler mixing rule includes one additional adjustable binary interaction parameter k_{12} besides the three parameters included in the

NRTL g^E model. These four adjustable parameters for PRSV-WS model were correlated from experimental vapor-liquid phase equilibrium data for water-THF mixture at constant temperature, available in the literature [27].

Dashtizadeh EOS is expressed by [25]:

$$Z = \frac{v+b}{v-b} - \frac{\alpha}{RT(v+b)} \quad (15)$$

In general, parameter a is considered as a function of reduced temperature and acentric factor and parameter b is considered constant. Parameter b is related to the volume of the molecules and plays an important role in the calculation of liquids densities. In liquid systems the intermolecular free volume is much smaller than that in the gas systems so in liquid systems parameter b is as important as parameter a. Therefore in Dashtizadeh EOS, parameter b is considered as a function of reduced temperature and acentric factor. This model with van der Waals mixing rule includes one adjustable binary interaction parameter k_{12}.

According to the SAFT EOS [26], the residual molar Helmholtz energy, a^{res}, has contributions from formation of hard sphere, chain, dispersion and association as follows:

$$\alpha^{res} = \alpha^{hs} + \alpha^{chain} + \alpha^{assoc} + \alpha^{disp} \quad (16)$$

In GV-SSAFT model, the Ghotbi–Vera EOS [26] was used as hard sphere contribution expressed by the following equation:

$$\alpha^{hs} = m(0.35\xi^8 + 0.4\xi^7 + 0.47\xi^6 + 0.56\xi^5 + 0.6\xi^4 + 0.452\xi^3 + 0.31\xi^2 - 3.14\xi - 6.1\ln(1-\xi))$$

$$(17)$$

With

$$\xi = \frac{\eta}{\tau} \quad , \quad \tau \frac{\pi\sqrt{2}}{6} \qquad (18)$$

where ξ and τ are normalized and close-packed reduced densities, respectively. η is the reduced density and can be written as:

$$\eta = \frac{\pi N_{Av} \rho m d^3}{6} \qquad (19)$$

In Eq. (19), ρ, d and N_{Av} are the molar density, temperature dependent diameter for segments and Avogadro number, respectively. The temperature-dependent diameter of segments, d, can be written as:

$$d = \left[\frac{\sqrt{2}v^{oo}}{N_{Av}} \right]^{\frac{1}{2}} \left[1 - C \exp\left[\frac{-3u^o}{kT} \right] \right] \qquad (20)$$

where C is a constant with value of 0.333. Dispersion Helmholtz energy for the SSAFT EOS can be written as follows:

$$\frac{\alpha^{disp}}{RT} = m Z_M \ln\left(\frac{v_s}{v_s + v^* Y} \right) \qquad (21)$$

Also, the chain contribution to the residual Helmholtz energy for SSAFT is expressed using the Wertheim association theory as:

$$\frac{\alpha^{chain}}{RT} = (1 - m) \ln(g^{hs}(d)) \qquad (22)$$

The radial distribution function (RDF) used in the GV-SSAFT EOS is expressed as:

$$g^{hs}(d) = 1 + 1.85\xi + 2.52\xi^2 + 2.86\xi^3 + \frac{3\xi^4}{1-\xi} - \frac{0.95\xi^7}{1-\xi} \qquad (23)$$

The association term in Eq. (24) can be written according to the following equation:

$$\frac{\alpha^{assoc}}{RT} = \sum_A \left[\left(\ln X^A - \frac{X^A}{2} \right) \right] + \frac{M}{2} \qquad (24)$$

where XA is mole fraction of association site A not bonded and can be presented as:

$$X^A = \left[1 + N_{Av\rho} \sum_B X^B \Delta^{AB} \right]^{-1} \qquad (25)$$

where Δ^{AB} is the association strength and can be given as:

$$\Delta^{AB} = g^{hs}(d) \left[\exp\left(\frac{\varepsilon^{AB}}{kT} \right) - 1 \right] d^a k^{AB} \qquad (26)$$

Here κ^{AB} and ε^{AB} are the association energy and volume for the interaction between association sites A and B. For the phase equilibrium calculations, the parameters of the GV-SSAFT EOS, i.e., m, v^∞, u^0 for all molecules and κ^{AB} and ε^{AB} for self-associating molecules should be determined. These adjustable parameters were correlated from fitting the SAFT-based EOS to the liquid density and vapor pressure experimental data for pure fluids by minimizing the following objective function:

$$O.F. = \frac{1}{N} \left(\sum_{i=1}^{N} \left| \frac{P_{Expt}^{sat} - P_{caic}^{sat}}{P_{Expt}^{sat}} \right| + \sum_{i=1}^{N} \left| \frac{\rho_{Expt}^{liq} - \rho_{caic}^{liq}}{P_{Expt}^{liq}} \right| \right) \qquad (27)$$

where N refers to the number of the experimental points.

The four-site 4C association scheme has been used for water [28], while tetrahydrofuran has been considered to be nonassociating [29]. The pure component parameters obtained in this work for GV-SSAFT EOS are summarized in Table 1. The interaction coefficients k_{ij} for water-THF mixture in the studied models are obtained by minimizing the average absolute pressure deviation (AAPD) between experimental and calculated vapor liquid equilibrium data. Table 2 reports the values of the adjusted parameters for the studied models.

$$\%AAPD = \frac{100}{N} \sum_{i=1}^{N} \left| \frac{\rho_{i,calc} - \rho_{i,expt}}{P_{i,expt}} \right| \qquad (28)$$

3. Results and Discussion

In this work, the conditions of equal chemical potential of water in the clathrate hydrate and the remaining phases are used to calculate the temperature and pressure of H_2-THF hydrate formation. By following Lattice Distortion model, reference chemical potential difference of binary hydrogen hydrate with THF is calculated using the experimental hydrate formation temperature and pressure data ([9], [10]). Fig. 1 compares calculated RCPD for H_2-THF hydrates using GV-SSAFT EOS for liquid phase.

Table 1. The value for the segment parameters used in the GV-SSAFT EOS.

Substance	m	v^-	u^0/K	ε^{AB}/K	κ^{AB}	Data Source
Water	1.850	7.127	196.833	574.116	0.094	[30]
THF	3.377	15.355	121.502	-	-	[30]

Table 2. The values of binary interaction parameters and %AAPD for studied EOS in THF + water mixture.

EOS	k_{ij}			%AAPD[a]
DPTG	-0.2407			17
PR	-0.2016			19
GV-SSAFT	-0.12			9
NRTL	Δg_{12} (J/mol)	Δg_{21} (J/mol)	α_{12}	1.1
	5431.34	6563.189	0. 5107	
PRSV-WS	τ_{12}	τ_{21}	α_{12}	k_{12}	6
	15.0430	4.0530	0.1822	-0.1316	

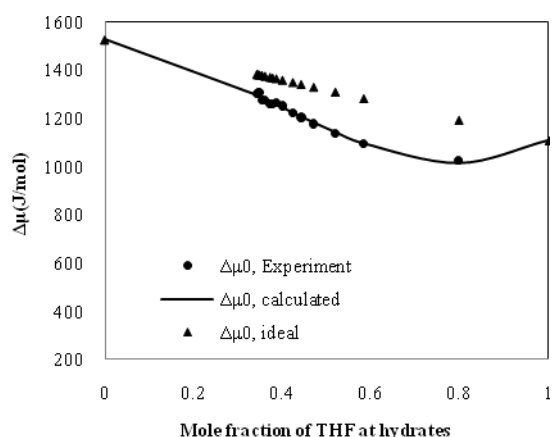a Experimental data are taken from reference [27].

Figure 1. RCPD of the THF-H$_2$ mixture determined by Florusse [9] and Lee data [10].

Constant A and B were correlated from binary hydrate experimental data by fitting experimental and calculated chemical potential to equation (8) for each studied model in liquid phase. The values for A and B are given in Table 3. Using the above correlated parameters, the dissociation pressure of H$_2$-THF hydrates at different temperatures can be calculated. Fig. 2 compares the correlated dissociation pressures with their experimental pressures as a function of temperature for five different studied models in liquid phase. The values of absolute relative deviation from experimental data for hydrate dissociation pressure of each studied thermodynamic model in liquid phase are given in Table 3. As shown in Table 3, the predicted pressure deviates considerably from the experimental values for NRTL model because contrary to the equations of state, this model does not consider the pressure effect in liquid phase on the fugacity. As can be seen from Table 3, the GV-SSAFT more accurately correlates the experimental hydrate dissociation pressure, especially at high pressure in H$_2$-THF in comparison to other studied thermodynamic models for liquid phase, because the GV-SSAFT considers the hydrogen bonding effect of water in liquid phase and also, the GV hard sphere EOS considers the limit of large molecules packing. In addition, among the studied cubic EOS, DPTG equation of state better correlates the experimental hydrate dissociation pressure due to taking the temperature dependence for parameter b in liquid phase into consideration.

Table 3. A and B parameters for the excess Gibbs potential model and the percent of AAPD for studied models in H$_2$+THF hydrates.

Model	A	B	Correlation Coefficient	%AAPD[a]
PR	-305.206	-798.604	0.9864	10.68
DPTG	-91.665	-498.5875	0.9905	6.70
NRTL	-955.849	-1525.179	0.9788	13.12
PRSV-WS	-1057.7	-1472.923	0.9842	12.61
GV-SSAFT	-641.984	-792.718	0.9975	4.95

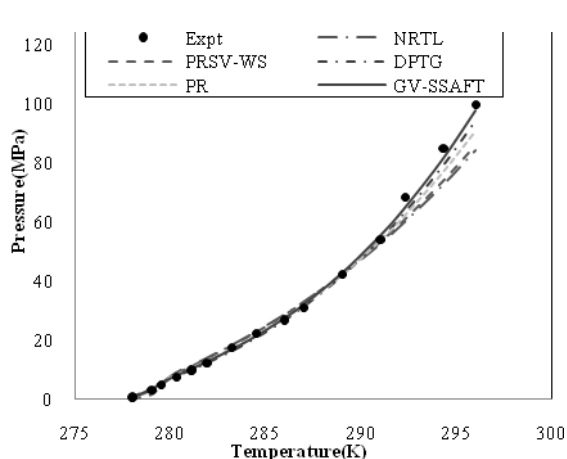a Experimental data are taken from references [9, 10].

Figure 2. Dissociation Pressure of the H_2+THF hydrates determined from experiments [9, 10] and prediction with Lattice Distortion model using the studied models.
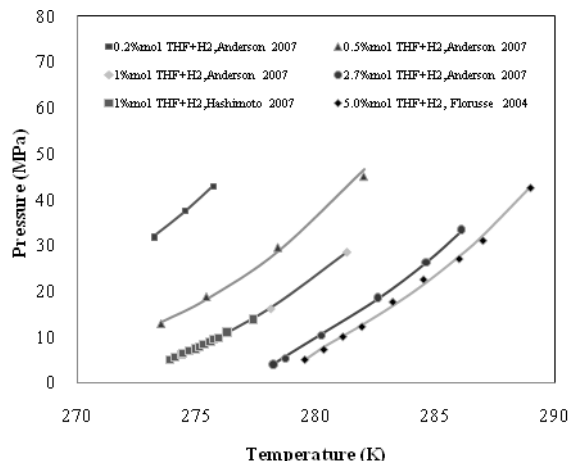

Figure 3. Dissociation Pressure of the H_2+THF hydrates for THF compositions not used in optimization with GV-SSAFT EOS.

As the GV-SSAFT model accurately correlated the dissociation pressure for THF-H_2 hydrate system at different temperatures in comparison with other liquid phase thermodynamic models, it is used to predict the dissociation pressure of H_2-THF hydrate system at different temperatures for the THF composition not included in optimization procedure ([9], [12], [31]).

Fig. 3 compares the GV-SSAFT model predictions for THF-H_2 hydrate at different THF concentrations with experimental values ([9], [12], [31]). It can be concluded from Fig. 3 that GV-SSAFT model accurately predicts the dissociation pressure of H_2-THF hydrate system.

The hydrogen and THF occupancies in the small and large cavities are also calculated using equation (3). Langmuir constant for hydrogen in equation (3) is calculated using Exp-6 potential model. Fig. 4 shows the variation of the hydrogen and THF occupancies in small and large cavities of
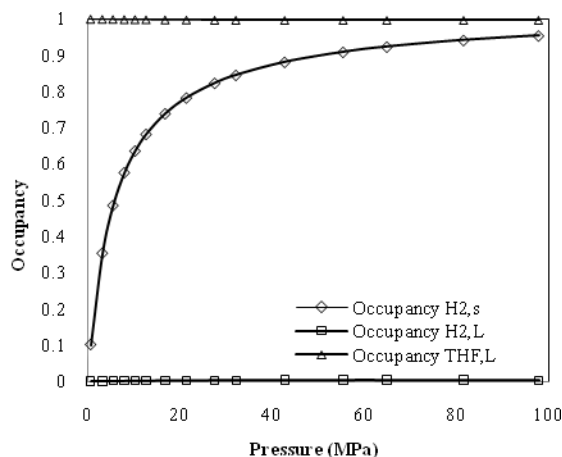

Figure 4. Occupancy of the small and large cavity by hydrogen and THF as a function of pressure.

hydrate as a function of pressure by GV-SSAFT EOS. As seen from Fig. 4, fractional occupancy of hydrogen in large cavity is very low and THF occupancy in large cavities is nearly constant and equal to 1 when THF concentration is near or equal to the stoichiometric concentration in hydrate. The occupancy of hydrogen in the small cages increases as pressure increases and at 100MPa reaches an occupancy value of 0.95.

Fig. 5 shows the variation of hydrogen content (as wt %) in THF-H₂ hydrate versus pressure. Since THF mostly occupies the large cavity, its hydrogen storage capacity is around 2wt% at 40MPa and reaches to 2.4wt% at 100MPa under 5 and 5.6 mole % of THF in the aqueous solution. This H2 content is very low and far away from the requirements for the practical application in H2 storage (the U.S. DOE target is set to 6.0 wt % by 2010 [32]). Calculated storage capacity in this work is in good agreement with experimental results of Florusse [9] and Lee [10] for H₂-THF hydrate system.
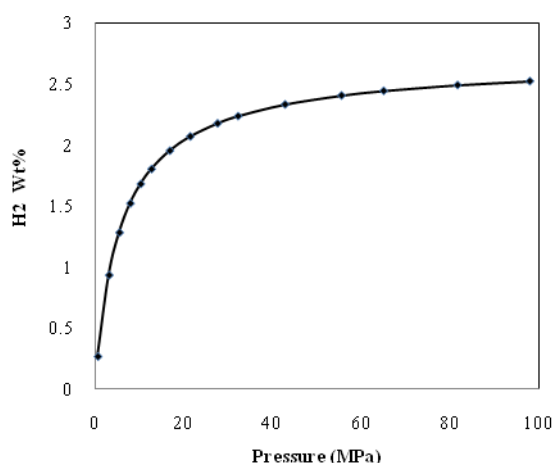

Figure 5. Hydrogen content as a function of pressure for binary H₂+THF hydrate using GV-SSAFT EOS.

4. Conclusions

Lattice Distortion model is used to account for changes in RCPDs due to the water cavity distortion of binary hydrates. This model predicts equilibrium condition of binary hydrogen hydrate with THF as a promoter. Four equations of state in addition to NRTL excess Gibbs free energy model are used for calculating the liquid phase fugacity in Lattice Distortion model. It was shown that the GV-SSAFT EOS correlates better with the experimental data of dissociation

pressure of H₂-THF hydrate system than those obtained using PR, PRSV-WS, DPTG EOSs, and also the NRTL model. It was also shown that the occupancy of hydrogen in small cavities at high pressures reaches to a maximum value of 0.95 and the large cavities are occupied mostly by THF.

Nomenclature

a	Helmholtz free energy
A,B	constant of equation 8
C	constant of equation 20 (0.333)
d	temperature-dependent diameter of segments
f_j	fugacity of component j
g^{hs}	radial distribution function
h	molar enthalpy j/mol
k	Boltzmann's constant j/K
m	number of segments
P	pressure
R	cavity radius
R	gas constant, j/(mol.K)
T	temperature
u_0	temperature independent square-well depth
v	molar volume cm³/mol
v^∞	segment molar volume in a closed-packed arrangement
x_w	Mole fraction of liquid water
X^A	mole fraction of component not bonded at site A
W	cell potential
z_i	Coordination number of cavity type i
Z_j	mole fraction of component j in hydrate phase

Greek Letters

α, β	Constant in equation 10
γ_w	activity coefficient of water

δ	polynomial defined by Equation 13
ε	depth of intermolecular potential well, j
ε^{AB}	volume for the interaction between association sites A and B
ξ	normalized reduced density
η	reduced density
θ_{ji}	fraction of cavities type i occupied by component j
μ	chemical potential, j/ mol
κ^{AB}	association energy for the interaction between association sites A and B
$\mu_w^H, \mu_w^L, \mu_w^{\beta}$	chemical potential of water in hydrate phase, liquid phase and empty hydrate, respectively, j/mol
υ_i	number of cavities type i per water molecule in hydrate
ρ	Molar density cm^3/mol
σ	distance parameter Å
τ	close-packed reduced density

Subscripts

calc	Calculated
expt	experimental
mix	mixture
w	water

Superscripts

0	property at ice point
assoc	association
disp	dispersion
hs	hard sphere
H	hydrate
L	Liquid
res	residual
sat	saturated

References

[1] Martin, A. and Peters, C.J., "Thermodynamic modeling of promoted structure, II clathrate hydrates of hydrogen", J. Phys. Chem., B 113, 7548, (2009).

[2] Profio, P.D., Arca, S., Rossi, F. and Flipponi, M., "Comparison of hydrogen hydrates with existing hydrogen", Int. J. Hydrogen Energy, 34(22), 9173, (2009).

[3] Sloan, E.D., Clathrate hydrates of natural gases, 3rd ed., CRC Press, Boca Raton, (2008).

[4] Takeuchi, F., Ohmura, R. and Yasuoka, K., "Statistical-thermodynamics modeling", Int. J. Thermophys., 30, 1838, (2009).

[5] Storbel, T., Koh, C.A. and Sloan, E.D., "Hydrogen storage properties of clathrate hydrate materials", Fluid. Phase. Equilib., 261, 382, (2007).

[6] Mao, W.L., Mao, H.K., Goncharov, A.F., Struzhkin, V.V., Guo, Q.Z., Hu, J.Z., Shu, J.F., Hemley, R.J., Somayazulu, M. and Zhao, Y.S., "Hydrogen clusters in clathrate hydrate", Science, 297, 2247, (2002).

[7] Dyadin, Y.A., Larionov, E.G., Ya. Aladko, E., Yu. Manakov, A., Zhurko, F.V., Mikina, T.V., Yu. Komarov, V. and Grachev, E.V., "Clathrate formation in water-noble gas (hydrogen) systems at high pressures", J. Struct. Chem., 40, 790, (1999).

[8] Mao, W.L. and Mao, H.K., "Hydrogen storage in molecular compounds", PNAS, 101, 708, (2004).

[9] Florusse, L.J., Peters, C.J., Schoonman, J., Hester, K.C., Koh, C.A., Dec, S.F., Marsh, K.N. and Sloan, E.D., "Stable low-pressure hydrogen clusters stored in a binary clathrate hydrate", Science, 306, 469, (2004).

[10] Lee, H., Lee, J.W., Kim, D.Y., Park, J., Seo, Y.T., Zeng, H., Moudrakovski, I.L., Ratcliffe, C.I. and Ripmeester, J.A., "Tuning clathrate hydrates for hydrogen storage", Nature, 434, 743, (2005).

[11] Strobel, T.A., Taylor, C.J., Hester, K.C., Dec, S.F., Koh, C. A., Miller, K.T. and Sloan, E.D., "Molecular hydrogen storage in binary THF−H_2 clathrate hydrates", J. Phys. Chem., B 110, 17121, (2006).

[12] Anderson, R., Chapoy, A. and Tohidi, B., "Phase relations and binary clathrate hydrate formation in the system H_2-THF-H_2O", Langmuir, 23, 3440, (2007).

[13] Hashimoto, S., Sugahara, T., Sato, H. and Ohgaki, K., "Thermodynamic stability of H_2+ Tetrahydrofuran mixed gas hydrate in nonstoichiometric aqueous solutions", J. Chem. Eng. Data, 52, 517 (2007).

[14] Lee, S.Y. and Holder, G.D., "A generalized model for calculating equilibrium states of gas hydrates: Part II", Ann. N.Y. Acad. Sci., 912, 614, (2000).

[15] Zele, S.R., Thermodynamic modeling of gas hydrates., Ph.D. Thesis, University of Pittsburgh, (1994).

[16] Lee, J.W., Yedlapalli, P. and Lee, S., "Prediction of hydrogen hydrate equilibrium by integrating ab initio calculations with statistical thermodynamics", J. Phys. Chem., B 110, 2332, (2006).

[17] Gibanel, F., Lopez, M.C., Royo, F.M., Santafe, J. and Urieta, J.S., "Solubility of nonpolar gases in tetrahydrofuran at 0 to 30 and 101.33 kPa partial pressure of gas", J. Solution Chem.,

22, 211, (1993).

[18] Holder. Corbin, G.D. and Papadopoulos, K. D., "Thermodynamic and molecular properties of gas hydrates from mixtures containing methane, argon, and krypton", Ind. Eng. Chem. Fundam., 19, 282, (1980).

[19] Sloan, E.D., Clathrate Hydrates of Natural Gases, 2nd ed., Marcel-Dekker, New York, (1998).

[20] Lee, S.Y., Yedlapalli, P. and Lee, J.W., "Excess Gibbs potential model for multi-component hydrogen clathrates", J. Phys. Chem., B 110, 26122, (2006).

[21] Danesh, A., PVT and phase behavior of petroleum reservoir fluids, Amsrterdam, (2003).

[22] Renon, H. and Prausnitz, J.M., "Local composition in thermodynamic excess function for liquid mixtures", AIChE J., 14, 135, (1968).

[23] Orbey, H. and Sandler, S.I., Modeling vapor–liquid equilibria, Cambridge University Press, New York, NY. (1998).

[24] Wong, S.H. and Sandler, S.I., "A theoretically correct mixing rule for cubic equations of state", AIChE J., 38, 671, (1992).

[25] Dashtizadeh, A., Pazuki, G.R., Taghikhani, V. and Ghotbi, C., "A new two-parameter cubic equation of state for predicting phase behavior", Fluid. Phase. Equilib., 242, 19, (2006).

[26] Asadi Malekshah, V., Taghikhani, V., Ramazani S.A., A. and Ghotbi, C., "Application of a new simplified SAFT to VLE study of associating and non-associating fluids", Fluid. Phase. Equilibr., 233, 110, (2005).

[27] Gmehling, J., Onken, U. and Arlt, W., Vapor–liquid equilibria data collection, DECHEMA, Vol.1, Pt. 1a., (1978).

[28] Gani, R., Muro-Sune, N., Sales-Cruz, M., Leibovici, C. and O'Connell, J. P., "Mathematical and numerical analysis of classes of property models", Fluid. Phase. Equilib., 250, 1, (2006).

[29] Giner, B., Royo, F.M., Lafuente, C. and Galindo, A., "Intermolecular potential model parameters for cyclic ethers and chloroalkanes in the SAFT-VR approach", Fluid. Phase. Equilibr., 255, 200, (2007).

[30] Green, D.W. and Perry, R.H., Perry's chemical engineers' Handbook, 8th ed., McGraw-Hill, New York, (2008).

[31] Hashimoto, S., Murayama, S., Sugahara, T., Sato, H. and Ohgaki, K., "Thermodynamic and Raman spectroscopic studies on H_2 + tetrahydrofuran + water and H_2+tetra-n-butyl ammonium bromide + water mixtures containing gas hydrates", Chem. Eng. Sci., 61, 7884, (2006).

[32] Papadimitriou, N.I., Tsimpanogiannis, I.N. and K.Stubos, A., "Gas content of binary clathrate hydrates with promoters", J. Chem. Phys., 131, 044102, (2009).